

SATB2 augments Δ Np63 α in head and neck squamous cell carcinoma

Jacky Chung^{1,2}, Joanne Lau², Lynn S. Cheng², R. Ian Grant², Fiona Robinson², Troy Ketela¹, Patricia P. Reis³, Olga Roche³, Suzanne Kamel-Reid³, Jason Moffat¹, Michael Ohh³, Bayardo Perez-Ordóñez⁴, David R. Kaplan^{1,2} & Meredith S. Irwin^{2,3,5+}

¹Department of Molecular Genetics, University of Toronto, ²Cell Biology Program, Hospital for Sick Children Research Institute, ³Department of Laboratory Medicine and Pathobiology, University of Toronto, ⁴Department of Pathology, University Health Network, and ⁵Department of Paediatrics, Hospital for Sick Children, Toronto, Ontario, Canada

Δ Np63 α is a critical pro-survival protein overexpressed in 80% of head and neck squamous cell carcinomas (HNSCCs) where it inhibits TAp73 β transcription of p53-family target genes, which is thought to increase HNSCC resistance to chemotherapy-induced cell death. However, the mechanisms governing Δ Np63 α function are largely unknown. In this study, we identify special AT-rich-binding protein 2 (SATB2) as a new Δ Np63 α -binding protein that is preferentially expressed in advanced-stage primary HNSCC and show that SATB2 promotes chemoresistance by enhancing Δ Np63 α -mediated transrepression by augmenting Δ Np63 α engagement to p53-family responsive elements. Furthermore, SATB2 expression positively correlates with HNSCC chemoresistance, and RNA interference-mediated knockdown of endogenous SATB2 re-sensitizes HNSCC cells to chemotherapy- and γ -irradiation-induced apoptosis, irrespective of p53 status. These findings unveil SATB2 as a pivotal modulator of Δ Np63 α that governs HNSCC cell survival.

Keywords: apoptosis; chemotherapy; p63; SATB2; SCC

EMBO reports (2010) 11, 777–783. doi:10.1038/embor.2010.125

INTRODUCTION

p63 and p73 are members of the p53 family of proteins that encode multiple isoforms by alternative splicing or alternative promoter usage (Flores, 2007). The latter generates transactivation-

competent (TA) or truncated, dominant-negative (Δ N) p63 and p73 that lack the amino (N)-terminal transactivation domain that is necessary for the induction of apoptosis and tumour suppression (Yang *et al*, 2002). Δ Np63 and Δ Np73 antagonize the activity of full-length TAp63 and TAp73, as well as p53, by forming abortive transcriptional tetramers that compete against TA-p53 family complexes for promoter-binding sites (Yang *et al*, 2002). In addition, Δ Np63 can directly activate transcription of genes involved in differentiation and development (Flores, 2007).

Unlike p53, p63 and p73 are rarely mutated or inactivated in human cancers. However, Δ Np63 and Δ Np73 are overexpressed in certain tumours, suggesting an oncogenic role for these truncated isoforms (Cam *et al*, 2006; Rocco *et al*, 2006). For example, the Δ Np63 α isoform is specifically upregulated in stratified squamous cell carcinoma (SCC), including those found in the lung and cervix (Hibi *et al*, 2000; Deyoung & Ellisen, 2007). Perhaps the most well-studied model is SCC of the head and neck (HNSCC), in which Δ Np63 α is upregulated in approximately 80% of cases (Hibi *et al*, 2000). Although the loss of p53 probably contributes to the malignant progression of HNSCC lesions (Forastiere *et al*, 2001), p53 is not inhibited by Δ Np63 α in HNSCC (Rocco *et al*, 2006). Instead, Δ Np63 α functions as an essential survival protein by specifically inhibiting the pro-apoptotic TAp73 β —the predominant p73 isoform expressed in HNSCC—and by repressing the transcription of target genes, such as *nox*a and *puma* (Rocco *et al*, 2006). Notably, DNA-damaging chemotherapeutic drugs have been shown to trigger apoptosis, in part, by downregulating Δ Np63 α in squamous epithelial and HNSCC cells (Zangen *et al*, 2005; Rocco *et al*, 2006). Furthermore, forced expression of Δ Np63 α promotes chemoresistance, suggesting that Δ Np63 α activity is a critical determinant of drug responsiveness (Sun *et al*, 2009). Although the vast majority of HNSCCs highly express Δ Np63 α , these tumours vary in their susceptibility to treatment modalities, indicating that unidentified pathways exist that influence Δ Np63 α function and cell survival (Hibi *et al*, 2000).

¹Department of Molecular Genetics, University of Toronto, 1 King's College Circle, Toronto, Ontario, M5S 1A8,

²Cell Biology Program, Hospital for Sick Children Research Institute, 555 University Avenue, Toronto, Ontario, M5G 1L7,

³Department of Laboratory Medicine and Pathobiology, University of Toronto, 1 King's College Circle, Toronto, Ontario, M5S 1A8,

⁴Department of Pathology, University Health Network, 200 Elizabeth Street, Toronto, Ontario, M5G 2C4, and

⁵Department of Paediatrics, Hospital for Sick Children, 555 University Avenue, Toronto, Ontario, M5G 1X8, Canada

+Corresponding author. Tel: +1 416 813 7654/ext. 2912; Fax: +1 416 813 5327; E-mail: meredith.irwin@sickkids.ca

Received 17 February 2010; revised 21 July 2010; accepted 26 July 2010; published online 10 September 2010

Special AT-rich-binding protein 2 (SATB2) is a member of the SATB family of transcription factors that was first identified in mammals as a gene involved in palatogenesis and craniofacial morphogenesis (Dobrev *et al*, 2006). In addition to important roles in development, recent evidence suggests that SATB member proteins might have significant roles in cancer biology (Han *et al*, 2008). The SATB2 homologue, SATB1, is overexpressed in a subset of breast cancers that exhibit increased invasiveness and more readily form xenograft tumours (Han *et al*, 2008). This homologue, SATB1, regulates the expression of specific sets of genes involved in breast cancer metastasis, including *erbB2* and *mmp3* (Han *et al*, 2008), and high SATB1 levels are associated with poor prognosis in breast tumours (Han *et al*, 2008). Similar to SATB1, SATB2 binds to AT-rich sequences in nuclear matrix attachment regions and regulates gene expression by arranging chromatin packing and organization (Dobrev *et al*, 2003, 2006). In addition, SATB2 can indirectly affect gene transcription by augmenting the activity of other transcription factors, such as Runx2 and activating transcription factor 4 (Dobrev *et al*, 2006), which suggests that SATB2 can mediate downstream target gene expression independently of its matrix attachment region-binding capability. However, the role of SATB2 in cancer is unclear. In this study, we identify SATB2 as the first modulator of p63 and provide evidence supporting the role of SATB2 in the determination of HNSCC chemotherapy sensitivity.

RESULTS AND DISCUSSION

SATB2 is expressed in HNSCC cells

To identify proteins that interact with p63 α and p73 α , SaOs-2 osteosarcoma cells stably expressing T7-tagged carboxy (C)-terminal regions of p63 α and p73 α were immunoprecipitated with T7 antibody. Mass spectroscopy identified SATB2 as a 100-kDa co-precipitating protein (data not shown). *satb2* transcripts were not expressed ubiquitously across multiple cell lines of different tissue, but were present in a subset of HNSCC cells (Fig 1A; data not shown). By contrast, *satb1* transcripts were not detected in any HNSCC cell lines tested through reverse transcriptase (RT)-PCR (Fig 1A; supplementary Fig S1A online). We next generated two polyclonal SATB2-specific antibodies (supplementary Fig S1B online), and determined that SATB2, but not SATB1, protein is expressed in HNSCC cell lines, which also expressed *satb2* transcript (Fig 1B; supplementary Fig S1C,D online). These results demonstrate that SATB2 is expressed in a subset of HNSCC-derived cell lines.

SATB2 is upregulated in advanced HNSCC tumours

We asked whether SATB2 was upregulated in patient-derived HNSCC tumour specimens. Approximately 50% of the tumour samples showed elevated *satb2* in comparison with non-neoplastic squamous epithelial samples, as determined by RT-PCR (Fig 2A). Consistent with the messenger RNA (mRNA) expression data, immunohistochemistry performed on sections derived from multiple sites, including the tongue (19), floor of the mouth (7), buccal mucosa (3) and gingiva (5), revealed negative SATB2 staining in normal squamous epithelium, whereas tumour tissues stained positively for SATB2 (Fig 2B). In the majority of samples tested, SATB2 was detected in both nuclear and cytoplasmic compartments of tumour cells and, interestingly, hyperplastic and dysplastic tissues displayed the most prominent nuclear SATB2

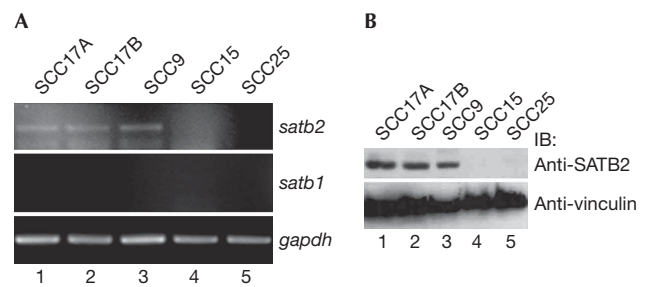


Fig 1 | Special AT-rich-binding protein 2 is expressed in a subset of HNSCC cells. (A) RT-PCR was performed on total RNA from the indicated HNSCC cell lines using the indicated primers. (B) SATB2 immunoblotting was performed on HNSCC whole-cell lysates. HNSCC, head and neck squamous cell carcinoma; RT-PCR, reverse transcriptase PCR; SATB2, special AT-rich-binding protein 2.

staining (Fig 2B). Positive anti-MIB1 staining, an antibody that detects the Ki67 proliferation marker, correlated with the most intense SATB2 and p63 staining (Fig 2B). Decreased levels of SATB2 were observed in tumour nests exhibiting more differentiated, keratinizing phenotypes and in the outer squamous epithelial layer (Fig 2B). In addition, SATB2 was most prominently expressed in the majority (17 of 22) of tongue HNSCC tumours with advanced pathological staging, whereas only a minority (7 of 21) of lower-stage tumours showed elevated SATB2 expression ($\chi^2 = 8.88$, d.f. = 2, $P < 0.05$; Fig 2C; supplementary Tables S1, S2 online). Notably, all 43 tumours showed positive p63 staining using a pan-p63 antibody, as Δ N-isoform-specific antibodies are not available for immunohistochemistry (data not shown).

Δ Np63 α and SATB2 form a stable complex *in vivo*

As Δ Np63 α is a critical pro-survival protein that is commonly overexpressed in HNSCC (Rocco *et al*, 2006), and we show that overlapping staining patterns of SATB2 and Δ Np63 α in HNSCC (Fig 2B), we asked whether SATB2 associates physically with Δ Np63 α . Flag- Δ Np63 α specifically precipitated with T7-SATB2 (Fig 3A), as well as endogenous SATB2 (supplementary Fig S2A online). In addition, T7-SATB2 precipitated with Flag-TAp63 α , but not TAp73 β (supplementary Fig S2B online; data not shown). Notably, a complex between SATB1 and p63 α was not observed in similar assays (supplementary Fig S2C,D online).

We next asked whether Δ Np63 α interacted physically with SATB2 under physiological conditions and observed that endogenous SATB2 specifically precipitated with Δ Np63 α in HNSCC cells (Fig 3B; supplementary Fig S1E online; Rocco *et al*, 2006). Furthermore, haemagglutinin-SATB2 and Flag- Δ Np63 α expressed in HeLa cells, as well as endogenous Δ Np63 α and SATB2 in SCC9 cells, co-localized in the nucleus, as shown by confocal immunofluorescence analysis (Fig 3C,D, respectively). These results suggest that Δ Np63 α and SATB2 form a stable complex *in vivo*.

Δ Np63 α recruits SATB2 to promoters

We next performed chromatin immunoprecipitation (ChIP) analysis by using SCC9 (p53 mutant) cells and SCC17A (p53 wild-type) cells to address whether SATB2 localizes to the

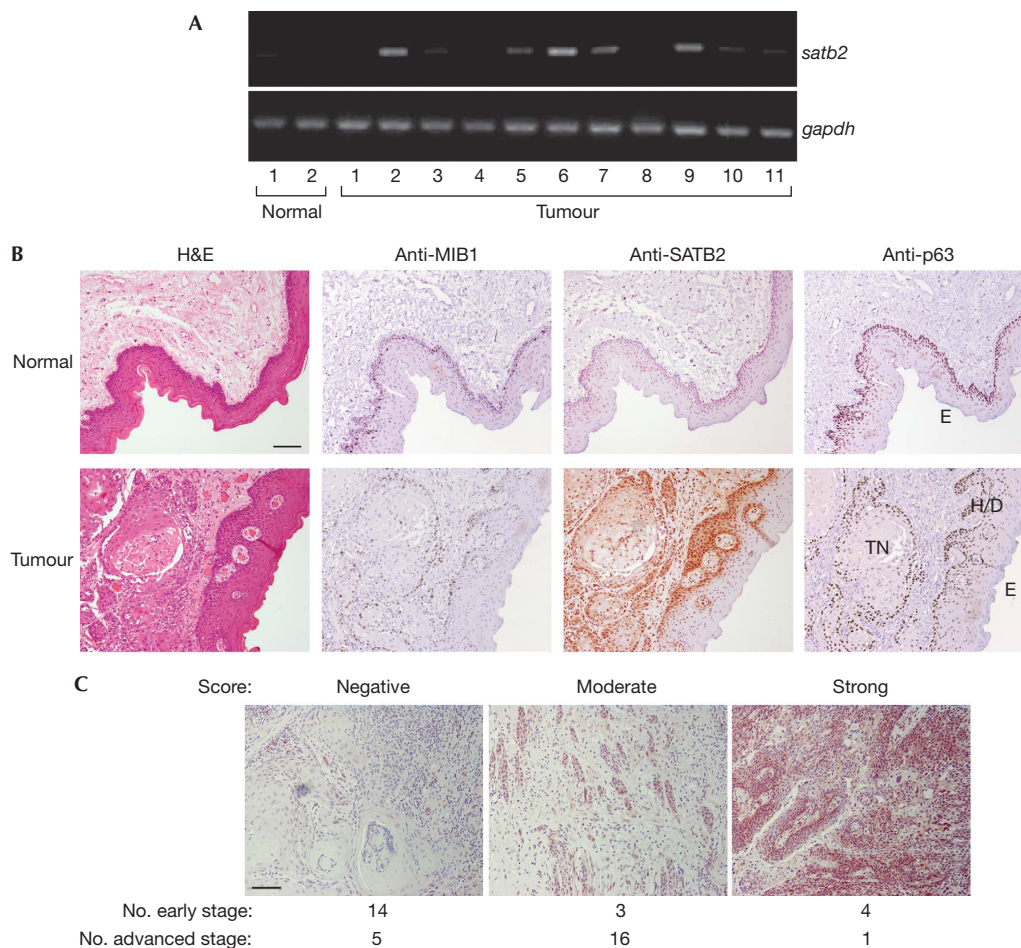


Fig 2 | Special AT-rich-binding protein 2 transcript and protein are detected in primary HNSCC tumours. (A) One microgram of total RNA isolated from HNSCC primary tumours (all of which are at advanced stage with the exception of tumour 6, which was early stage) was used for semi-quantitative RT-PCR using the indicated primers. (B) Representative paraffin-embedded human tongue HNSCC sections were stained with haematoxylin and eosin (top panels) and the indicated antibodies. (C) Forty-three tongue tumour specimens immunostained with SATB2-C-terminal antibody were scored as negative, moderate or strong. The numbers of early- and advanced-stage specimens are indicated under the representative images of each scoring category. Scale bar, 100 μ m. E, outer squamous epithelium; H/D, hyperplastic and dysplastic; HNSCC, head and neck squamous cell carcinoma; RT-PCR, reverse transcriptase PCR; SATB2, special AT-rich-binding protein 2; TN, tumour nests.

cis-acting DNA elements of p53-family target genes. Endogenous SATB2 localized on p53-family responsive elements recognized by Δ Np63 α , including *puma*, *pig3-1*, *pig3-2*, *hdm2*, *bax* and *perp* (Fig 4A,B; supplementary Fig S3A online). Sequential ChIP:reChIP analysis showed that endogenous Δ Np63 α and SATB2 co-localized on *puma* and *hdm2* promoters, but not on the non-p53 *gapdh* promoter (Fig 4C). Furthermore, SATB2 was only detected on target gene promoters in HCT116 (*p53*^{-/-}) cells, which also lack p63 expression, in the presence of ectopic Δ Np63 α expression (supplementary Fig S3B online). In addition, analysis of the indicated p53-family target genes using an algorithm designed to identify SATB-family DNA-binding consensus did not reveal any SATB-binding sites within 2 kb of the p53-family responsive elements (data not shown). A 2-kb interval was used in our analysis because the resolution of our ChIP analysis was less than 1 kb (data not shown). Notably, the algorithm reliably predicted SATB-family consensus sequences

previously identified in the promoters of genes, such as *mmp3* and *cln1* (Han et al, 2008; data not shown). Previous research has shown that SATB2 might regulate gene expression indirectly by interacting with other transcription factors, such as Runx2 and activating transcription factor 4 (Dobrev et al, 2006). Our results, here, suggest that SATB2 might function similarly and is recruited by Δ Np63 α to p53-family target promoter regions. In accord, ChIP analysis using primary *p63*^{-/-} mouse embryonic fibroblasts showed that endogenous SATB2 readily localized on the murine *p21* and *perp* promoters only in the presence of Flag- Δ Np63 α (Fig 4D). Although direct comparison with *p63*^{+/+} mouse embryonic fibroblasts was not feasible with available reagents due to low basal endogenous Δ Np63 α levels, endogenous SATB2 was detected on the *perp* promoter in *p63*^{+/+} murine brain lysates (supplementary Fig S3A online).

We next asked whether SATB2 influences the ability of Δ Np63 α to bind to p53-family responsive elements. HaCat cells,

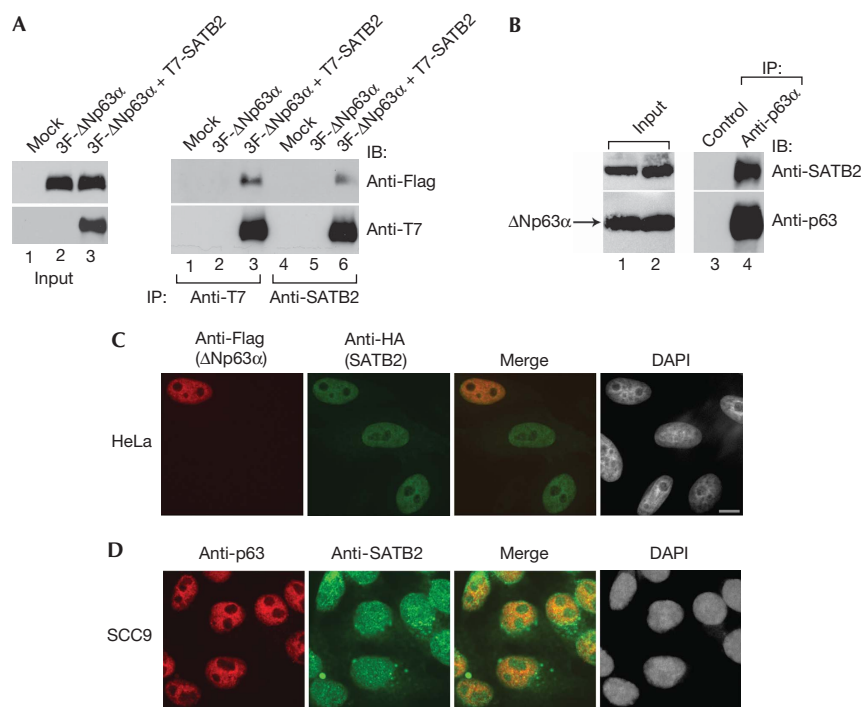


Fig 3 | Δ Np63 α and special AT-rich-binding protein 2 form a molecular complex *in vivo*. (A) HEK293 cells transiently transfected with the indicated expression plasmids were lysed and immunoprecipitated with the indicated antibodies. This was followed by anti-Flag immunoblotting. (B) SCC17A (p53 wild-type) lysates were immunoprecipitated and analysed by using immunoblotting with the indicated antibodies. (C) Transiently transfected HeLa cells were fixed and analysed by using confocal fluorescence microscopy with the indicated antibodies. (D) SCC9 (p53 mutant) cells were stained with the indicated antibodies and DAPI, and visualized using confocal fluorescence microscopy. Scale bar, 10 μ m. DAPI, 4',6-diamidino-2-phenylindole; HEK, human embryonic kidney; IB, immunoblotting; IP, immunoprecipitation; SATB2, special AT-rich-binding protein 2; SCC, squamous cell carcinoma.

which express no detectable SATB2 transcript or protein (Fig 4E, right panel; data not shown), were transduced with adenovirus-expressing green fluorescent protein (Ad-GFP) or SATB2 (Ad-SATB2). Real-time ChIP analysis showed that SATB2 significantly increased the engagement of Δ Np63 α on several indicated p53-family responsive elements (Fig 4E). Conversely, SCC9 cells with stable knockdown of endogenous SATB2 exhibited markedly reduced Δ Np63 α and SATB2 binding to p53-family target gene promoters (Fig 4F). SATB2 did not affect Δ Np63 α stability (supplementary Fig S4A,B online), suggesting that the effect of SATB2 on Δ Np63 α DNA binding was not due to changes in Δ Np63 α expression level. Furthermore, SATB2 enhanced the ability of Δ Np63 α to inhibit TAp73 β -mediated PG13 (13 contiguous p53-family responsive elements) reporter activation in HCT116 (p53^{-/-}) colon and H1299 (p53^{-/-}) lung adenocarcinoma cells in a dosage-dependent manner (Fig 4G; data not shown, respectively). These results suggest that SATB2 promotes the binding of Δ Np63 α to p53-family target gene promoters to repress gene expression.

SATB2 promotes chemoresistance in HNSCC

Δ Np63 α and TAp73 β have critical roles in HNSCC cell survival and chemosensitivity irrespective of p53 status (Zangen *et al*, 2005; Rocco *et al*, 2006). Consistent with these findings, cisplatin—one of the chemotherapeutic agents commonly used in the treatment of HNSCC—induced downregulation of Δ Np63 α

and concomitant induction of TAp73 β , and cleaved poly (ADP-ribose) polymerase, a marker of apoptosis, in SCC9 and other HNSCC cell lines (Fig 5A; data not shown). We show here that SATB2 augments the recruitment of Δ Np63 α to p53-family target gene promoters and that SATB2 is frequently overexpressed in advanced HNSCCs that are typically more chemoresistant. Thus, we asked whether SATB2 expression correlated with HNSCC chemosensitivity. The SCC25 cells that do not exhibit SATB2 expression were more sensitive to cisplatin and displayed lower survival levels and lethal dose 50 (LD₅₀) values over a range of doses correspondingly lower than SATB2-expressing SCC9 and SCC17A cells (Fig 5B; Table 1). Interestingly, SCC17A and SCC9 cells had similar LD₅₀ values, indicating that p53 status is not a strong indicator of cisplatin responsiveness (Table 1).

We next asked whether SATB2 directly promoted chemoresistance. The SCC9 and SCC17A cells with SATB2 knockdown through lentivirus-expressing SATB2-specific short hairpin RNA or small interfering RNA transfection, respectively, were much more susceptible to cisplatin-induced death in comparison with SCC9 cells infected with GFP- or shGFP-expressing lentiviruses, which had only modest, non-specific effects on protein expression, including SATB2 (Fig 5C–E; data not shown). Furthermore, SATB2 knockdown in SCC9 cells decreased viability in response to 5-fluorouracil and γ -irradiation in comparison with control SCC9 cells (supplementary Fig S5A,B online). We therefore hypothesized that a reduction in SATB2 levels would compromise

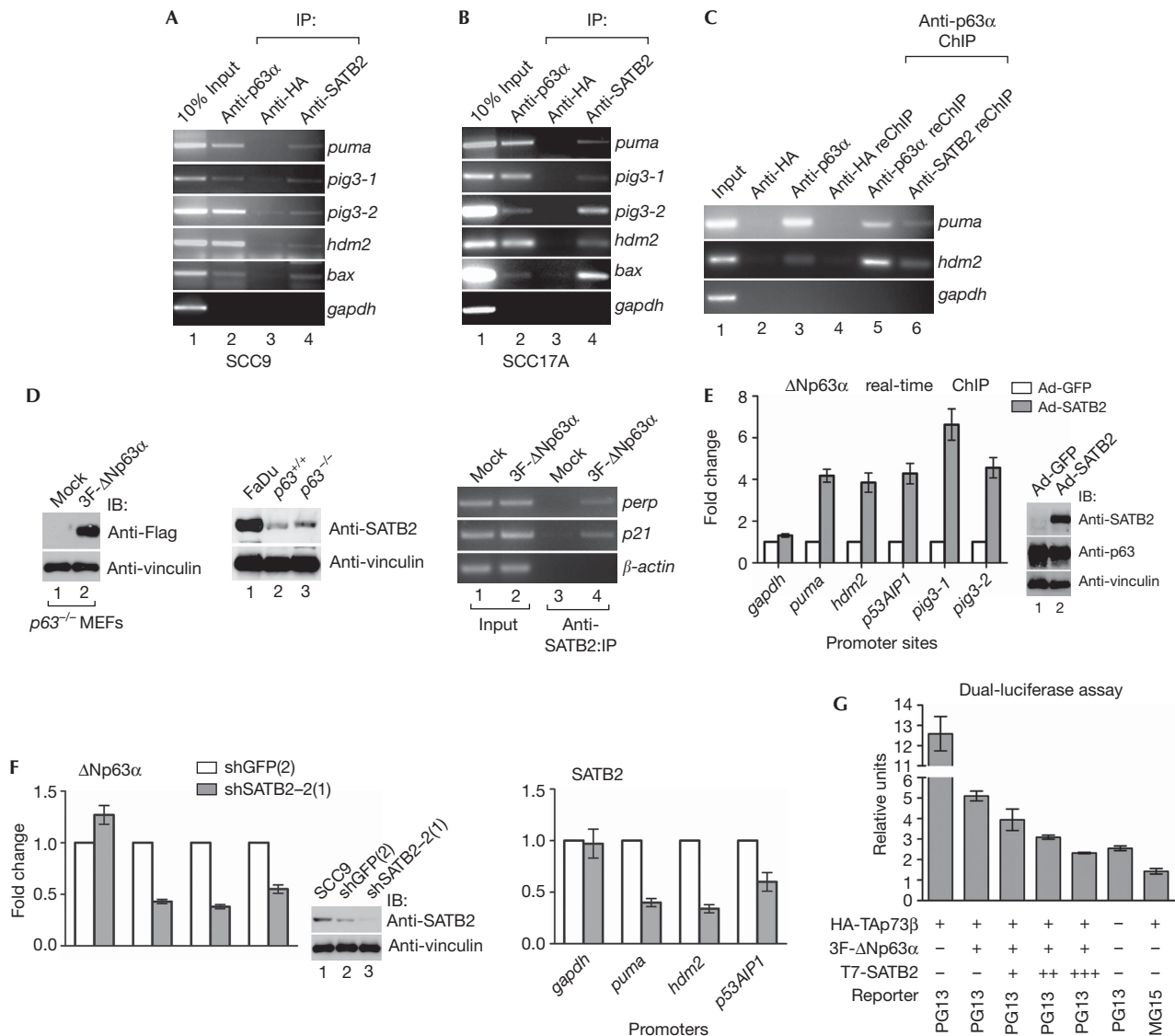


Fig 4 | Special AT-rich-binding protein 2 engages p53-family promoters through Δ Np63 α and augments Δ Np63 α -mediated transrepression. (A,B) SCC9 (p53 mutant) and SCC17A (p53 wild-type) cells were analysed by using ChIP with indicated antibodies, and PCR was performed using p53-family responsive-element-specific primers for the indicated genes. (C) Sequential ChIP:reChIP was performed on SCC17A cells using the indicated antibodies. (D) SATB2 ChIP analysis was performed on *p63*^{-/-} MEFs transfected with the indicated plasmids using primers specific for p53-family responsive elements targeting murine promoters (bottom panel). Levels of Δ Np63 α and endogenous SATB2 were confirmed in *p63*^{-/-} and *p63*^{+/+} MEFs (FaDu SCC cells are positive control; top right panel). (E) Real-time Δ Np63 α ChIP analysis was performed on HaCat cells infected with adenoviruses (Ad) encoding GFP (open bars) or SATB2 (grey bars) using primers for p53-family responsive elements in the indicated promoters. Results were normalized to the *gapdh* promoter input. Representative experiments (mean \pm s.d.) performed three independent times in quadruplicate are shown. The expression of endogenous Δ Np63 α and Ad-transduced SATB2 was confirmed through western blot analysis (right panels). (F) Real-time Δ Np63 α ChIP analysis was performed on SCC9 cells stably expressing shGFP (clone 2) (open bars) or shSATB2-2 (clone 1) (grey bars). Results were normalized to the input level of each individual gene promoter. The graph shows data from one representative experiment (mean \pm s.d.). (G) Δ Np63 α -mediated inhibition of TAp73 β was analysed by performing PG13-luciferase assays on HCT116-*p53*^{-/-} cells transfected with various combinations of HA-TAp73 β and 3F- Δ Np63 α with increasing amounts of T7-SATB2 (0.024, 0.24 and 2.4 μ g). A representative experiment performed in triplicate is shown (mean \pm s.d.). ChIP, chromatin immunoprecipitation; GFP, green fluorescent protein; HA, haemagglutinin; MEF, mouse embryonic fibroblast; SATB2, special AT-rich-binding protein 2; SCC, squamous cell carcinoma; sh, short hairpin; WT, wild type.

Δ Np63 α transrepression activity and consequently lead to TAp73 β -mediated transactivation of apoptotic genes. Consistent with this idea, cisplatin treatment of SCC9 cells with stable knockdown of SATB2 showed enhanced levels of *puma*, *nox*a and

Bax as compared with cells expressing SATB2 (Fig 5F; supplementary Fig S5C,D online). These results demonstrate that SATB2 enhances cell survival in the presence of radiation and chemotherapeutic agents.

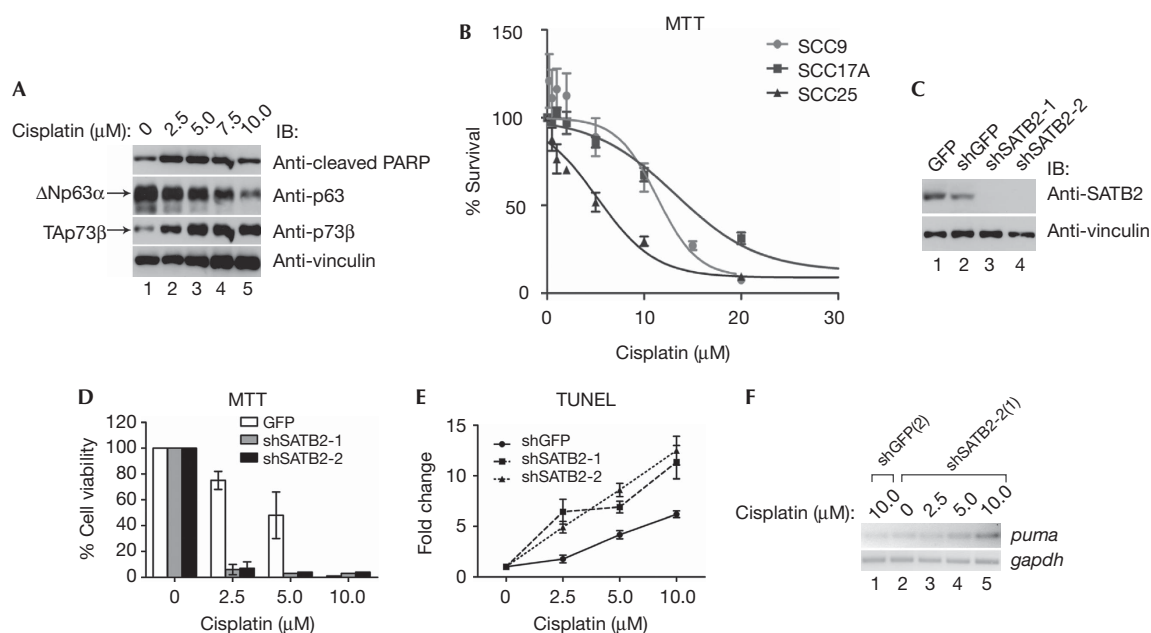


Fig 5 | Special AT-rich-binding protein 2 promotes radioresistance and chemoresistance of HNSCC cells. (A) SCC9 (p53 mutant) cells treated with cisplatin were subjected to cleaved-PARP, p63 and p73 β immunoblotting. (B) MTT assay was performed on SATB2-positive SCC9 (circles) and SCC17A (squares) cells, and SATB2-negative SCC25 cells (triangles) treated with cisplatin. Data from one representative experiment are shown ($n = 3$, mean \pm s.d.). (C) Lysates of SCC9 cells transiently infected with GFP-, shGFP- or SATB2-specific shRNAs (shSATB2-1 and -2) lentiviruses were lysed and analysed by immunoblotting. (D) MTT assay was performed on cisplatin-treated SCC9 cells infected with GFP (open bars), shSATB2-1 (grey bars) or shSATB2-2 (black bars) lentiviruses and scored relative to untreated cells. Error bars represent mean \pm s.d. from four data points in a representative experiment. (E) Indicated lentivirus-infected SCC9 cells treated with cisplatin were analysed by TUNEL staining. Fold changes were normalized to the untreated cells. Error bars represent mean \pm s.d. from five fields of view of a representative experiment. (F) Stable SCC9 cells expressing the indicated shRNAs were treated with indicated cisplatin doses and semi-quantitative RT-PCR was performed with the indicated primers. GFP, green fluorescent protein; HNSCC, head and neck squamous cell carcinoma; MTT, 3-(4,5-dimethylthiazol-2-yl)-2,5-diphenyltetrazolium bromide; RT-PCR, reverse transcriptase PCR; SATB2, special AT-rich-binding protein 2; SCC, squamous cell carcinoma; shRNA, short hairpin RNA; TUNEL, terminal deoxynucleotidyl transferase-mediated dUTP-biotin nick end labelling.

SATB2 has an important role in development (Dobrova *et al*, 2006; Alcamo *et al*, 2008). However, a role for SATB2 in cancer or apoptosis has not, until now, been described. In the progression model of HNSCC, dysplasia and hyperplasia represent precursor lesions that progress, on accumulation of additional genetic alterations, into malignant and invasive carcinomas (Forastiere *et al*, 2001). The prominent expression of SATB2 observed in hyperplastic/dysplastic regions suggests that SATB2 overexpression constitutes an early step in oncogenesis, similar to the role of SATB1 in breast cancer (Forastiere *et al*, 2001; Han *et al*, 2008). This idea is consistent with the highly proliferative, undifferentiated, non-keratinizing cells located at the periphery of tumour nests showing the most intense SATB2 staining in comparison with more differentiated, keratinizing nests often displaying negligible SATB2 staining. Interestingly, downregulation of SATB2 and Δ Np63 during differentiation of primary keratinocytes has been reported (Pozzi *et al*, 2009). Our findings that SATB2 is preferentially expressed in advanced HNSCC tumours and has modulatory effects on the p53-family protein, Δ Np63 α , help to explain the resistance of late-stage HNSCC to common cancer treatments. In addition to primary tumour data, the use of multiple cancer cell lines and primary cells highlights the physiological

Table 1 | LD₅₀ values for HNSCC cell lines with varying SATB2 expression

| Cell line | p53 status | SATB2 expression | LD ₅₀ (μ M)* |
|-----------|------------|------------------|------------------------------|
| SCC9 | Mutant | Positive | 11.6 \pm 0.2 |
| SCC17A | Wild type | Positive | 11.8 \pm 0.8 |
| SCC25 | Mutant | Negative | 6.6 \pm 0.8 |

*Mean \pm s.e.m., $n = 3$.
HNSCC, head and neck squamous cell carcinoma; LD₅₀, lethal dose 50; SATB2, special AT-rich-binding protein 2.

significance of our results. DeYoung *et al* (2006) have shown that, in contrast to normal keratinocytes, HNSCC cells are uniquely dependent on Δ Np63 α for survival, which further supports Δ Np63 α and modulators, such as SATB2, that augment Δ Np63 α -anti-apoptotic function as new therapeutic targets. Ultimately, drugs targeting key players in p53-family signalling pathways might translate into improved therapies and prognoses for patients with advanced-stage HNSCC and other cancers that exploit the p63/p73 network (DeYoung & Ellisen, 2007; Leong *et al*, 2007).

METHODS

Immunohistochemistry. Research Ethics Board Approval at University Health Network (Toronto) was obtained for tumour analyses. Immunohistochemistry was performed as previously described (Dos Reis *et al*, 2008). The SATB2 staining intensity was scored as previously described for SATB1 (Han *et al*, 2008) with modifications (see supplementary information online).

RT-PCR. A total of 1 µg of total RNA, isolated using the RNeasy kit (Qiagen, Germantown, MD, USA), was used for reverse transcription with the Omniscript RT kit (Qiagen). The PCR amplification was performed as described under ChIP with an annealing temperature of 55 °C except for *puma* (60 °C) and *nox* (50 °C). See supplementary information online for primer sequences and expected PCR product sizes.

Dual-Luciferase, MTT and TUNEL assays. Luciferase assays were performed using the Dual-Luciferase Reporter Assay System (Promega, Madison, WI, USA) according to the manufacturer's instructions. At 3 days after infection, cells were seeded (8.0×10^3 – 1.0×10^4 cells per well) in 96-well plates and, 24 h later, treated with the indicated drugs for 48 h in quadruplicate. 3-(4,5-dimethylthiazol-2-yl)-2,5-diphenyltetrazolium bromide (MTT) cell proliferation assay (Roche Applied Science, Brandford, CT, USA) was carried out according to the manufacturer's instructions. Data analysis was carried out using GraphPad Prism 5.0 (GraphPad Software, La Jolla, CA, USA; mean \pm s.e.m., $n = 3$). After infection, SCC9 cells were seeded (5.0×10^4 cells per well) in a 12-well plate. 137 Cesium was used as a γ -irradiation source and, 48 h later, affixed onto Shandon Double Coated Cytoslides (Thermo Scientific Corporation, Waltham, MA, USA). Terminal deoxynucleotidyl transferase-mediated dUTP-biotin nick end labelling (TUNEL) staining was performed using the DeadEnd Fluorometric TUNEL System (Promega). Percentage apoptosis was scored by dividing the number of green, TUNEL-positive nuclei by the total number of 4',6-diamidino-2-phenylindole-stained nuclei (five fields of view per experiment, $n = 3$).

See supplementary information online for additional materials and methods.

Supplementary information is available at EMBO reports online (<http://www.emboreports.org>).

ACKNOWLEDGEMENTS

This study was supported by funds from Canadian Cancer Society (018054) and the Cancer Research Society. J.C. is a recipient of a Doctoral Canada Graduate Scholarship from Canadian Institutes of Health Research. M.O., D.R.K. and M.S.I. are Canada Research Chairs.

We thank A. Marzotto for assistance with the development of SATB DNA-binding sites algorithm.

CONFLICT OF INTEREST

The authors declare that they have no conflict of interest.

REFERENCES

- Alcama EA, Chirivella L, Dautzenberg M, Dobrova G, Farinas I, Grosschedl R, McConnell SK (2008) Satb2 regulates callosal projection neuron identity in the developing cerebral cortex. *Neuron* **57**: 364–377
- Cam H *et al* (2006) p53 family members in myogenic differentiation and rhabdomyosarcoma development. *Cancer Cell* **10**: 281–293
- Deyoung MP, Ellisen LW (2007) p63 and p73 in human cancer: defining the network. *Oncogene* **26**: 5169–5183
- DeYoung MP, Johannessen CM, Leong CO, Faquin W, Rocco JW, Ellisen LW (2006) Tumor-specific p73 up-regulation mediates p63 dependence in squamous cell carcinoma. *Cancer Res* **66**: 9362–9368
- Dobrova G, Dambacher J, Grosschedl R (2003) SUMO modification of a novel MAR-binding protein, SATB2, modulates immunoglobulin mu gene expression. *Genes Dev* **17**: 3048–3061
- Dobrova G, Chahrouh M, Dautzenberg M, Chirivella L, Kanzler B, Farinas I, Karsenty G, Grosschedl R (2006) SATB2 is a multifunctional determinant of craniofacial patterning and osteoblast differentiation. *Cell* **125**: 971–986
- Dos Reis PP, Bharadwaj RR, Machado J, Macmillan C, Pintilie M, Sukhai MA, Perez-Ordenez B, Gullane P, Irish J, Kamel-Reid S (2008) Claudin 1 overexpression increases invasion and is associated with aggressive histological features in oral squamous cell carcinoma. *Cancer* **113**: 3169–3180
- Flores ER (2007) The roles of p63 in cancer. *Cell Cycle* **6**: 300–304
- Forastiere A, Koch W, Trotti A, Sidransky D (2001) Head and neck cancer. *N Engl J Med* **345**: 1890–1900
- Han HJ, Russo J, Kohwi Y, Kohwi-Shigematsu T (2008) SATB1 reprogrammes gene expression to promote breast tumour growth and metastasis. *Nature* **452**: 187–193
- Hibi K, Trink B, Patturajan M, Westra WH, Caballero OL, Hill DE, Ratovitski EA, Jen J, Sidransky D (2000) AIS is an oncogene amplified in squamous cell carcinoma. *Proc Natl Acad Sci USA* **97**: 5462–5467
- Leong CO, Vidnovic N, DeYoung MP, Sgroi D, Ellisen LW (2007) The p63/p73 network mediates chemosensitivity to cisplatin in a biologically defined subset of primary breast cancers. *J Clin Invest* **117**: 1370–1380
- Pozzi S, Zambelli F, Merico D, Pavesi G, Robert A, Maltere P, Gidrol X, Mantovani R, Vigano MA (2009) Transcriptional network of p63 in human keratinocytes. *PloS One* **4**: e5008
- Rocco JW, Leong CO, Kuperwasser N, DeYoung MP, Ellisen LW (2006) p63 mediates survival in squamous cell carcinoma by suppression of p73-dependent apoptosis. *Cancer Cell* **9**: 45–56
- Sun Q, Ming L, Thomas SM, Wang Y, Chen ZG, Ferris RL, Grandis JR, Zhang L, Yu J (2009) PUMA mediates EGFR tyrosine kinase inhibitor-induced apoptosis in head and neck cancer cells. *Oncogene* **28**: 2348–2357
- Yang A, Kaghad M, Caput D, McKeon F (2002) On the shoulders of giants: p63, p73 and the rise of p53. *Trends Genet* **18**: 90–95
- Zangen R, Ratovitski E, Sidransky D (2005) DeltaNp63alpha levels correlate with clinical tumor response to cisplatin. *Cell Cycle* **4**: 1313–1315